



## A quantitative method for evaluating cortical responses to electrical stimulation

Lawrence J. Crowther<sup>a</sup>, Peter Brunner<sup>a,b</sup>, Christoph Kapeller<sup>c</sup>, Christoph Guger<sup>c</sup>,  
Kyousuke Kamada<sup>d</sup>, Marjorie E. Bunch<sup>b</sup>, Bridget K. Frawley<sup>b</sup>, Timothy M. Lynch<sup>b</sup>,  
Anthony L. Ritaccio<sup>a,b,f</sup>, Gerwin Schalk<sup>a,b,e,\*</sup>

<sup>a</sup> National Center for Adaptive Neurotechnologies, Wadsworth Center, New York State Department of Health, Albany, NY, USA

<sup>b</sup> Department of Neurology, Albany Medical College, Albany, NY, USA

<sup>c</sup> g.tec Guger Technologies OG, Graz, Austria

<sup>d</sup> Department of Neurosurgery, Asahikawa Medical University, Asahikawa, Japan

<sup>e</sup> Department of Biomedical Sciences, State University of New York at Albany, Albany, NY, USA

<sup>f</sup> Department of Neurology, Mayo Clinic, Jacksonville, FL, USA

### ARTICLE INFO

#### Keywords:

Cortico-cortical evoked potentials  
Electrical stimulation  
Electrocorticography  
Connectivity

### ABSTRACT

**Background:** Electrical stimulation of the cortex using subdurally implanted electrodes can causally reveal structural connectivity by eliciting cortico-cortical evoked potentials (CCEPs). While many studies have demonstrated the potential value of CCEPs, the methods to evaluate them were often relatively subjective, did not consider potential artifacts, and did not lend themselves to systematic scientific investigations.

**New method:** We developed an automated and quantitative method called SIGNI (Stimulation-Induced Gamma-based Network Identification) to evaluate cortical population-level responses to electrical stimulation that minimizes the impact of electrical artifacts. We applied SIGNI to electrocorticographic (ECoG) data from eight human subjects who were implanted with a total of 978 subdural electrodes. Across the eight subjects, we delivered 92 trains of approximately 200 discrete electrical stimuli each (amplitude 4–15 mA) to a total of 64 electrode pairs.

**Results:** We verified SIGNI's efficacy by demonstrating a relationship between the magnitude of evoked cortical activity and stimulation amplitude, as well as between the latency of evoked cortical activity and the distance from the stimulated locations.

**Conclusions:** SIGNI reveals the timing and amplitude of cortical responses to electrical stimulation as well as the structural connectivity supporting these responses. With these properties, it enables exploration of new and important questions about the neurophysiology of cortical communication and may also be useful for pre-surgical planning.

### 1. Introduction

Research over the past few decades has identified the functional organization of the human brain in unprecedented detail (De Beeck et al., 2008), revealing a tight relationship between particular brain regions and specific motor, perceptual, or cognitive functions (e.g., Schalk et al., 2017). At the same time, it remains unclear how these regions are anatomically connected to each other. Indeed, neither of the two currently available methods for discovering the anatomical connections between different brain regions — diffusion tensor imaging (DTI) or resting-state functional magnetic resonance imaging (fMRI)

correlations — enable unambiguous conclusions about point-to-point structural connectivity in the human brain (Assaf and Pasternak (2008) and Smith et al. (2013), respectively). This ambiguity in establishing anatomical connectivity in humans impedes exploration of many basic neuroscientific questions as well as planning for invasive brain surgeries.

Identifying the location of cortical responses to direct electrical stimulation of the human brain can provide undisputable evidence for direct or indirect structural connectivity between them, and identifying the temporal sequence of those responses (which is not possible using DTI or resting-state fMRI) can add directional information. Indeed,

\* Corresponding author.

E-mail addresses: [crowther@neurotechcenter.org](mailto:crowther@neurotechcenter.org) (L.J. Crowther), [gschalk@neurotechcenter.org](mailto:gschalk@neurotechcenter.org) (G. Schalk).

<https://doi.org/10.1016/j.jneumeth.2018.09.034>

Received 25 July 2018; Received in revised form 5 September 2018; Accepted 6 September 2018

Available online 04 October 2018

0165-0270/ © 2018 Published by Elsevier B.V.

early implementations of this technique, commonly termed cortico-cortical evoked potentials (CCEPs), have been used in many investigations to study connectivity in a variety of human brain networks in vivo for quite some time (Matsumoto et al., 2004). For example, studies evaluated aspects of the auditory system (Howard et al., 2000; Brugge et al., 2003; Oya et al., 2007), language system (Matsumoto et al., 2004; Umeoka et al., 2009; Conner et al., 2011; Koubeissi et al., 2011; Keller et al., 2011; Enatsu et al., 2013a; David et al., 2013; Entz et al., 2014; Yamao et al., 2014; Saito et al., 2014; Araki et al., 2015; Tamura et al., 2016), and visual system (Matsuzaki et al., 2013). Other studies identified connectivity in the motor system (Matsumoto et al., 2007; Terada et al., 2008, 2012; Kikuchi et al., 2012; Swann et al., 2012; Enatsu et al., 2013b), limbic system (Wilson et al., 1990, 1991; Catenoix et al., 2005; Rosenberg et al., 2008; Umeoka et al., 2009; Koubeissi et al., 2013; Almashaikhi et al., 2014; Lacuey et al., 2015; Jiménez-Jiménez et al., 2015; Enatsu et al., 2015), and connectivity with and within the frontal lobe (Lacruz et al., 2007; Matsumoto et al., 2012; Greenlee et al., 2004, 2007; Garell et al., 2012). Finally, a few studies compared connectivity identified with CCEPs to connectivity identified using resting state fMRI (Keller et al., 2011), resting-state broadband gamma correlations (Keller et al., 2014a, 2014b), and diffusion tensor imaging (DTI) (Donos et al., 2016).

The CCEP studies described above provided early evidence for the utility of electrical stimulation for identifying connectivity, but also suffered from three distinct issues. First, almost all of them relied on identification of traditional evoked potentials (ERPs), but the physiological origin and morphology of ERPs is complex and relatively undefined (Makeig et al., 2002; Mazaheri and Jensen, 2006, 2008; Kam et al., 2016). For example, CCEP studies to date described a seemingly large variety of different ERP components resulting from electrical stimulation. Initial reports described an early negative potential (N1) occurring at 10–50 ms, and a later potential (N2) occurring at 50–300 ms (Matsumoto et al., 2004). More recent studies also describe positive potentials (P1 and P2) that precede and follow the N1, respectively (Araki et al., 2015). These different ERP features greatly impede standardized quantification, physiological interpretation, and temporal localization of CCEPs. Please see Discussion for further information on this topic. Second, most previous studies relied on visual inspection and subjective interpretation for identifying the spatial location of CCEPs or their features, which impedes systematic investigations and widespread scientific and clinical application of this technique. Third and relatedly, electrical stimulation of the cortex is likely to produce electrical artifacts (stimulation amplitudes are on the order of volts whereas recorded ERPs are on the order of microvolts), both immediately at the time of stimulation but also afterwards due to capacitive effects, that may masquerade as physiological responses to electrical stimulation. Prior attempts to address this issue range from excluding channels with large artifacts identified by visual inspection (Formaggio et al., 2013) to template-matching based on electrical modeling of the electrode-tissue interface (Trebaul et al., 2016). Together, these three issues impose substantial limitations on the

neuroscientific advances or clinical benefits that could be enabled by widespread implementation and rigorous application of the CCEP technique.

In this paper, we introduce a new method for evaluating cortical connectivity called SIGNI (Stimulation-Induced Gamma-based Network Identification) that has three features, each addressing one of the issues described above. The first feature is our use of electrocorticographic (ECoG) activity in the broadband gamma (70–170 Hz) range. In contrast to traditional ERPs, ECoG broadband gamma has become widely accepted as a key indicator of cortical population-level activity (Voytek et al., 2010; Crone et al., 2001; Darvas et al., 2010; Edwards et al., 2010, 2005, 2009; Chang et al., 2011; Jensen et al., 2007; Maris et al., 2011; Ray et al., 2008; Tort et al., 2008; Wang et al., 2010), i.e., a direct reflection of the average firing rate of neurons directly underneath the electrode (Miller et al., 2009; Whittingstall and Logothetis, 2009; Manning et al., 2009; Ray and Maunsell, 2011), and has been shown to drive the BOLD signal identified using fMRI (Logothetis et al., 2001; Mukamel et al., 2005; Niessing et al., 2005; Engell et al., 2012; Hermes et al., 2012). Thus, the use of broadband gamma enables more precise physiological interpretations and, when used in conjunction with recently developed methods (Coon et al., 2016; Coon and Schalk, 2016), allows for highly precise temporal localization of cortical activation at specific locations and in single trials. The second feature is our development and validation of rigorous signal processing steps and statistical tests that support completely automated, quantitative, and objective evaluation of broadband gamma responses to electrical stimulation. Third, SIGNI includes an artifact removal procedure that minimizes the possibility that results are driven by electrical artifacts rather than physiological responses.

We validated SIGNI using ECoG activity from eight human subjects while we stimulated the cortex with a total of 92 trains of discrete electrical stimuli (median of 200 stimuli each). Our results document the expected relationship between distance between stimulating and responding sites and ECoG broadband latency ( $r^2 = 0.4$ ,  $p < 0.01$ ), as well as the amplitude of electrical stimulation and the overall magnitude of ECoG broadband responses ( $r^2 = 0.4$ ,  $p < 0.05$ ). Together with its strong physiological basis, we expect that the automated and quantitative nature of SIGNI will enable comprehensive and rigorous studies of structural connections in the human brain.

## 2. Methods

### 2.1. Subjects

Eight human subjects (A–H) requiring electrical stimulation mapping prior to tumor resection (subject B) or surgical resection of epileptogenic tissue (all other subjects) participated in this study. The Institutional Review Boards of Albany Medical College (Albany, New York) and Asahikawa Medical University (Asahikawa, Hokkaido, Japan) approved the study, and all subjects provided informed written consent. All subjects had normal cognitive capacity and were

**Table 1**  
Clinical profile, electrode array specifications, and stimulation parameters for each subject.

Subject	Age	Sex	Grid locations	Electrode diameter (mm)	Electrode pitch (mm)	# Electrodes	# Stimulation trains	Current amplitude (mA)
A	53	F	right frontal, parietal, temporal	3	10	86	6	4, 8
B	49	F	left frontal, parietal	3	10	64	4	5, 10
C	57	M	right frontal, parietal, temporal	3	6, 10	138	12	6, 10
D	25	M	left occipital, parietal	3	10	88	8	5, 10
E	33	M	left temporal, frontal, parietal, hippocampus	1, 3	3, 10	232	13	5, 10, 15
F	26	F	right temporal, frontal, parietal	1.5, 3	5, 10	144	33	10, 15
G	51	M	left temporal, frontal, parietal, mesial	3	10	126	9	10
H	36	F	right temporal, frontal, parietal, mesial	3	6, 10	100	7	10

functionally independent. Clinical profiles for each subject are summarized in Table 1.

Subjects were implanted with subdural electrode arrays (PMT Corporation, Chanhassen, MN or Unique Medical Co., Tokyo, Japan); electrodes had an exposed diameter of 1–3 mm and were spaced 3–10 mm apart. The number of implanted electrodes ranged from 64 to 232 (978 total). Across all subjects, we obtained coverage of left and right temporal, frontal, parietal, and left occipital cortices as well as the hippocampus (in subject E). Electrode arrays were surgically implanted for approximately one week (or intraoperatively in the case of subject B) and location varied according to clinical indication. During data collection for this study, each subject was awake, but rested and did not actively participate in any task. Electrode coverage and implant duration was dictated solely by the requirements of the clinical procedure without consideration of the research study.

We utilized preoperative MRI imaging to produce three-dimensional brain models with Freesurfer (<http://surfer.nmr.mgh.harvard.edu>) for anatomically accurate visualization. In extraoperative cases, we localized implanted electrodes through co-registration of post-operative computer tomography (CT) scans using SPM (<http://www.fil.ion.ucl.ac.uk/spm>). In the intraoperative case, we determined the location of visible electrode contacts with MRI-based neuronavigation (Brainlab AG, Munich, Germany). We extrapolated the location of electrodes that were not visibly exposed from neighboring visible contacts.

## 2.2. Cortical response detection and evaluation

The SIGNI procedure for detecting and evaluating cortical activity induced by electrical stimulation is graphically outlined in Fig. 1 and summarized below. First, we generated discrete electrical stimuli with a current-controlled cortical stimulator (S12X (Grass Technologies Corporation, West Warwick, Rhode Island) or MS-120-EEG (Nihon Kohden Corporation, Irvine, California)). Stimuli were biphasic or alternating monophasic waveforms with frequency 1–2 Hz, pulse width 300  $\mu$ s, and current amplitudes ranging from 4 to 15 mA (Fig. 1A). During stimulation, we recorded ECoG signals from all except the stimulated electrodes using g.HIamp hardware (g.tec medical engineering GmbH, Austria) and general-purpose brain-computer interface software

BCI2000 (Schalk et al., 2004; Schalk and Mellinger, 2010). The g.HIamp has 24-bit analog-to-digital converters and uses oversampling to increase the signal-to-noise ratio to observe broadband gamma activity. Recorded signals were amplified and digitized at 4800 Hz in parallel to the clinical monitoring system to ensure that clinical data collection was uninterrupted. We identified the timing of stimulation events by submitting the TTL trigger output of the stimulator to the g.HIamp recording hardware via g.TRIGbox hardware (g.tec medical engineering GmbH, Austria); the g.HIamp digitized the trigger output in sync with the ECoG signals. We delivered stimuli to electrodes of interest by avoiding epileptogenic foci (see the lateral radiograph in Fig. 1B for typical electrode coverage). In the present study, we delivered trains of electrical stimuli (a median of 200 stimuli per train) to each cortical target and repeated these stimulation trains with different current amplitudes.

We high-pass filtered recorded signals at 0.1 Hz to remove drift and applied a common average reference (CAR) filter to minimize signal noise as shown in Fig. 1C. The voltage amplitude used in electrical stimulation can be in the range of several to tens of volts. The amplitude of the raw ECoG signal is on the order of tens of microvolts, and broadband gamma signals may have even smaller amplitudes. Thus, electrical stimulation introduces instantaneous and, due to analog circuitries in the amplifier, longer-lasting artifacts in the recorded ECoG signals. Importantly, these artifacts may appear at sites distant to the stimulated sites due to charge transfer across the cortex. Hence, proper evaluation of physiological responses to electrical stimulation implies that it is essential to remove or minimize these electrical artifacts. This issue is not trivial, because: (1) the band-pass filtering necessary to extract broadband gamma signals can distribute artifactual signals around the time of stimulation; (2) simple approaches to artifact removal (e.g., deleting ECoG data during stimulation) produces discontinuous signals that again produce artifacts during subsequent band-pass filtering; and (3) anodic stimulation creates artifacts that are different from cathodic stimulation, and cortical stimulators usually apply both. To address these issues, we developed an automated artifact removal and feature extraction procedure (Fig. 1D). To remove the primary stimulation artifact, we replaced the artifactual ECoG data during the time of stimulation (0–5 ms) with stationary ECoG data whose

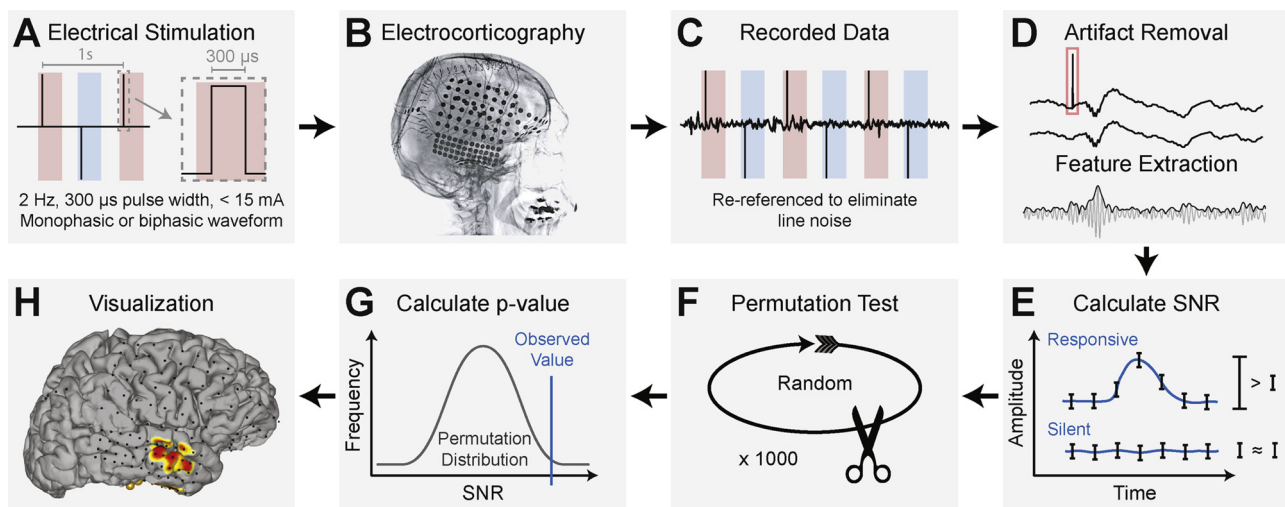


**Fig. 1.** Method for automated quantification of neural activity elicited by direct electrical stimulation of the cortex. (A) A cortical stimulator generates electrical stimuli with a specified frequency, pulse duration, current amplitude, and waveform. Red and blue periods indicate alternating anodic and cathodic stimulation. (B) Electrical stimuli are delivered to cortical targets underlying implanted subdural electrodes that are shown in this lateral radiograph. (C) Electroencephalographic (ECoG) signals are recorded from the electrodes with high sampling frequency. (D) Stimulation artifacts, as indicated by the red rectangle, are removed and broadband gamma signals (amplitudes in the 70–170 Hz band) are extracted. (E) The signal-to-noise ratio in a post-stimulus period is calculated with the method described in Schalk et al. (2007). (F) A permutation test is performed to generate a distribution of SNR values that would be expected if no cortical response to stimulation occurred. (G) A  $p$ -value is calculated for each channel based on the observed SNR value and the permutation distribution. (H) Resulting  $p$ -values are corrected for multiple comparisons and are visualized using NeuralAct software (Kubaneck and Schalk, 2015).

amplitude and spectral distribution was the same as that of background ECoG signals. To do this, we removed the immediate stimulation artifacts, and replaced it with a tapered copy of the reversed preceding and following ECoG signal. Specifically, we copied and reversed the ECoG signals from  $-5$  to  $0$  ms, and multiplied by a vector defined as  $1:1/n:0$ , where  $n$  is the number of samples in the  $5$  ms period. Second, we copied and reversed the data from  $5$  to  $10$  ms, and multiplied it by a second vector, defined as  $0:1/n:1$ . We then added the two resulting time series together and used it to replace the ECoG time series from  $0$  to  $5$  ms (i.e., the time containing the primary stimulation artifact). To remove longer-lasting artifacts, and those specific to anodic vs. cathodic stimulation, we then subtracted from the resulting time series the average time series<sup>1</sup> (separate for anodic vs. cathodic stimulation trials) for each electrode from each trial. Finally, we extracted broadband gamma signals by applying a zero-phase non-causal band-pass filter (8th-order Butterworth) between  $70$  and  $170$  Hz, and computed the absolute value of the Hilbert transform of these band-pass filtered results.

Fig. 2 gives exemplary signals that summarize the principal steps of our artifact removal and feature extraction procedure. First, the main stimulation artifact on a channel is presented ( $\pm 50$  mV) in Fig. 2A. This artifact is different for trials using anodic and cathodic stimulation (red and blue traces, respectively), and can be as much as three orders of magnitude larger than the broadband gamma signals we seek to detect. Fig. 2B shows average time courses for this channel after removal of the main artifact. Fig. 2C shows raw ECoG time courses after subtraction of the corresponding average trial. Fig. 2D gives the broadband gamma signals in the  $70$ – $170$  Hz range; they are in the  $\pm 50$   $\mu$ V amplitude range.

We then identified those cortical locations whose broadband gamma signals increased in amplitude after the stimulus using the signal-to-noise (SNR) procedure described in Schalk et al. (2007), (Fig. 1E). This procedure is highly sensitive to amplitude modulations following the stimulus and relates the variance across a defined response detection period,  $\sigma^2(f)$ , to the average variance of shorter subdivided periods,  $\frac{1}{n} \sum_{i=1}^n \sigma^2(f_i)$ , resulting in a single SNR value for each electrode. If the signal at a given electrode is temporally modulated by the stimulus, then the variance of the whole period (across trials) will exceed the average variance of the bins it is comprised of, resulting in an SNR value larger than  $1$ . Conversely, if the variance of the whole period is similar to that of the bins, the stimulus has not modulated the signal's amplitude in the considered period, resulting in an SNR value of close to  $1$ . In the present study, we calculated SNR values using ECoG broadband signals between  $10$  and  $100$  ms post stimulus (six consecutive  $15$  ms bins).

We then determined, at each location, whether the corresponding SNR value was statistically different from  $1$ , i.e., the value expected if there was no stimulus-related ECoG broadband modulation (Fig. 1F). To do this, we applied a randomization test in which we repeated the SNR calculation  $1000$  times<sup>2</sup> after reversing the ECoG broadband

<sup>1</sup> For each channel, we calculated the coefficient of determination ( $r^2$ ) to express the extent to which the variance of broadband gamma amplitude at the time of its peak is accounted for by the stimulus. Comparing these values with and without removal of an averaged trial demonstrates the value of this processing step. Specifically, for each responding channel in every trial, we considered the average amplitude in a  $10$  ms period prior to the stimulus and a  $10$  ms period centered on the time of the average response peak. In  $5$  of  $8$  subjects, we found that removal of the averaged time series statistically increased this coefficient of determination (paired-sample  $t$ -test,  $p \ll 0.01$ ), i.e., increased the signal-to-noise ratio of the resulting signal, when comparing the signals with and without the subtraction procedure. The remaining  $3$  subjects had fewer responding locations and results were not significantly different between the conditions, but all three showed improvements in average  $r^2$  ( $0.017$ ,  $0.003$ , and  $0.002$ , respectively).

<sup>2</sup> Preliminary testing established that  $1000$  permutations provided essentially

signals in each trial and applying a circular shift at a randomly selected interval. This produced a distribution of SNR values that represented no significant modulation of broadband gamma activity in the post-stimulus period.

We determined the statistical significance of post-stimulus broadband gamma changes at each electrode by applying the observed SNR value to a normal cumulative distribution function calculated from the permutation distribution of log-normalized SNR values for each channel (Fig. 1G). We applied a Kolmogorov–Smirnov test to ensure that the permutation distribution accurately modeled a normal distribution (Massey, 1951), and Bonferroni-corrected the resulting  $p$ -values to account for multiple comparisons. Finally, we visualized the magnitude of broadband gamma modulation by topographically mapping the negative log of the Bonferroni-corrected  $p$ -values with NeuralAct software (Kubaneck and Schalk, 2015) (Fig. 1H).

### 2.3. Validation of the artifact removal procedure

Determining the presence/absence of stimulation artifacts is a daunting problem, because there is no simple and definitive test to evaluate whether an observed response is physiological or artifactual. Nevertheless, we are confident that the procedure described above produces results that are at most only minimally affected by electrical artifacts, because we conducted extensive qualitative and quantitative tests during development and validation. To test this procedure qualitatively, we carefully visually inspected signals before and after artifact removal. As a demonstrative example, Fig. 3A gives ECoG signals without (red trace) and with (green trace) artifact removal. The red trace indicates a prominent response close to the time of stimulation, and a smaller response that peaks around  $40$  ms. Because the first response occurs immediately with stimulation (which is unlikely if it were a physiological response) and because it is completely absent in the green trace, it is almost certainly a stimulus-related electrical artifact that is completely removed by our artifact removal procedure.

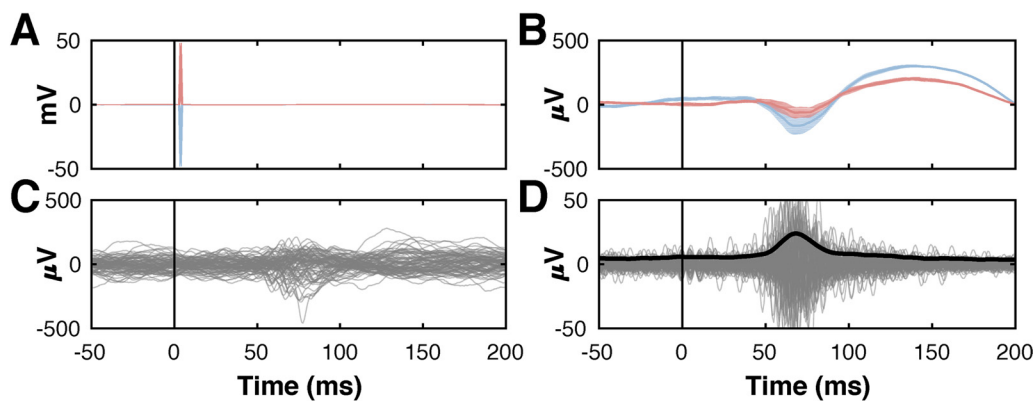
We also tested our artifact removal procedure quantitatively by evaluating its effect on the measurements of the (expected) relationship between the distance between stimulated and responding sites, and the latency of the activity onset. (Since it is difficult to determine the length of the fiber tracts between two locations, we used the Euclidean distance. Even though the Euclidean distance is only a proxy of the true distance between the two locations, the latency of the ECoG response should still be a function of the distance.) To establish the latency of the ECoG broadband gamma response, we modeled average ECoG broadband gamma amplitudes in the  $200$  ms prior to the stimulus with a normal distribution and then determined the first time after the stimulus at which the average ECoG amplitude exceeded the voltage corresponding to  $\alpha = 0.001$ . Fig. 3B shows red circles at the distance and activity onset at each responding site for subject F without artifact removal. These results indicate a weak relationship ( $r^2 = 0.10$ ) between distance and activity onset. They include many data points for which activity onset is close to  $0$  irrespective of distance, which is physiologically implausible. Artifact removal dramatically increases the relationship between distance and activity onset ( $r^2 = 0.42$ ), and eliminated all datapoints with a latency close to  $0$ , Fig. 3C. In sum, our qualitative and quantitative validation efforts indicated that artifacts due to electrical stimulation had at most a minimal effect on our results.

## 3. Results

We measured two expected aspects of stimulus-related cortical activity to test the utility of SIGNI. First, we established that the aggregate

(footnote continued)

the same result as  $10,000$  permutations, consistent with earlier findings by Coon and Schalk (2016).



gamma (70–170 Hz) range (gray traces) ( $\pm 50 \mu\text{V}$ ), and their average envelope (black trace), highlighting a physiological response around 70 ms.

**Fig. 2.** Demonstration of artifact removal and feature extraction procedure using ECoG from a location that shows a broadband gamma response to cortical stimulation. (A) Averaged ECoG signal with prominent stimulation artifact ( $\pm 50 \text{ mV}$ ). Red and blue traces indicate responses resulting from anodic and cathodic stimulation (alternating monophasic stimulation), respectively. (B) Averaged signals trials after removal of the immediate electrical artifact. (C) Individual trials following subtraction of the corresponding average trial. (D) Band-pass filtered ECoG signals in the broadband

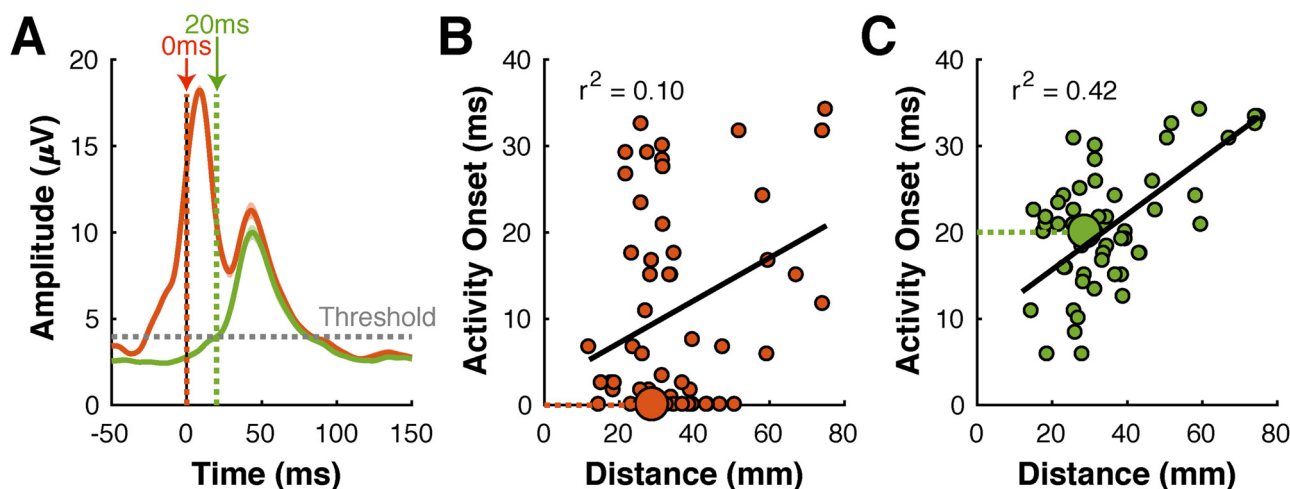


**Fig. 3.** Effect of artifact removal on results. (A) Broadband gamma time courses from a single location in subject F. Green/red traces represent signals with/without application of the artifact removal process, respectively. The red trace, but not the green trace, shows a prominent stimulation artifact at the time of stimulation. (B) Relationship between distance between stimulated and responding site, and the onset of the broadband gamma response. Each dot represents results for one combination of stimulated and responding site. The larger dot represents data for the responding site shown in (A). Several data points suggest an onset time close to 0 irrespective of distance to the stimulating site. Relationship between distance and onset time is modest ( $r^2 = 0.10$ ). (C) Same data as in (B), except that signals were processed with the artifact removal process. Onset times are at least several ms, and relationship between distance and onset time is greatly improved ( $r^2 = 0.42$ ).

magnitude of the cortical response to electrical stimulation is a function of the stimulation amplitude. Second, we determined how the distance from the stimulated sites affects the onset of stimulus-related cortical activity.

### 3.1. Effect of current amplitude

We first hypothesized that increasing stimulation amplitude will increase the number of responding cortical locations and/or their response amplitude. Fig. 4 gives an example from subject C that is consistent with this hypothesis. In this example, only four locations (marked by blue dots in panel A) produce detectable responses at 6 mA, but 18 locations (the 4 blue locations and 14 additional red locations) produce responses for stimulation at 10 mA (Fig. 4A). Overall, we stimulated six different locations at these two stimulation amplitudes in this subject. Cortical response magnitude (defined here as the cumulative SNR across all responding locations for a given specified stimulation location and current amplitude) increases with increased current (Fig. 4B,  $p < 0.05$ , paired-sample  $t$ -test). The blue and red dots indicate results for the stimulation/responding locations shown in panel A.

We find the same effect also across all subjects. Because stimulus amplitudes were different for different stimulus locations and across subjects, we grouped current amplitude as low (4–6 mA), medium (8–10 mA), and high (15 mA). We found that stimulation at medium

and high levels were significantly larger than stimulation at low levels (two-sample  $t$ -test,  $p < 0.01$ ), but we did not detect a significant difference between the medium and high current groups ( $p \gg 0.05$ ). This result suggests that, at least using our stimulation protocol, there appears to be at threshold current amplitude, and that stimulation beyond that amplitude does not increase cortical response magnitude. Further analysis with data obtained from stimulation at a range of current amplitudes is needed to further investigate this saturation threshold.

### 3.2. Effect of distance

We also hypothesized that the latency of ECoG broadband gamma responses increases with increasing Euclidean distance to the stimulation site. Fig. 5 shows exemplary data from stimulation of a location in the temporal lobe in subject F. Stimulation of the site marked with the lightning symbol in Fig. 5A elicited ECoG broadband activity at three locations marked with 1–3, respectively. The distance of each of these three sites to the stimulation site was 14 mm, 34 mm, and 75 mm, respectively. Fig. 5B gives broadband gamma time courses for these three locations; these time courses peaked at 43 ms, 54 ms, and 68 ms, respectively. This relationship between distance and latency was also present across subjects. See Fig. 6 for activity onset for groups of electrodes at different distances.

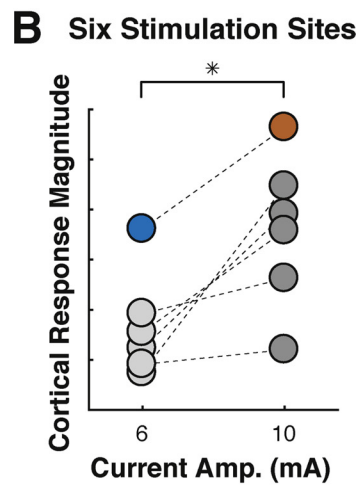
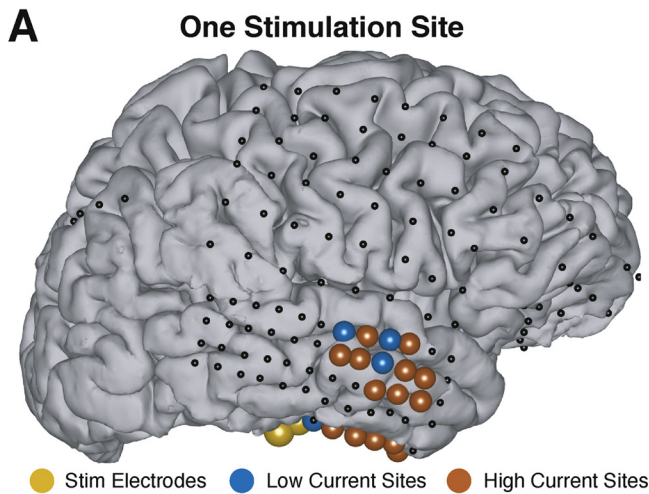


Fig. 4. Higher current amplitude increases stimulus-related cortical activity. (A) Example topography demonstrating stimulation location (yellow), locations responsive to low current amplitude (blue circles), additional locations only responsive to high current amplitude (red circles), and locations with no significant response (black dots). (B) Stimulating six cortical locations at 10 mA (instead of 6 mA) increased cortical response magnitude (paired-sample *t*-test,  $p < 0.05$ ). Data for the stimulation site shown in (A) is represented by the blue/red data points.

4. Discussion

Existing methods for determining cortical connectivity have distinct limitations. In this paper, we describe SIGNI, the first automated and quantitative method that can begin to address these limitations by evaluating cortical responses to direct electrical stimulation of the cortex. We applied our method to eight subjects to determine the amplitude and timing of cortical responses, which revealed that higher current amplitude increases cortical response magnitude, and that the latency of evoked population-level cortical activity increases with the distance from the stimulation site. Together, our results demonstrate the utility of SIGNI, and also suggest that stimulation artifacts have at most a negligible effect on our results. SIGNI provides the spatial and temporal progression of activation of cortical populations that causally result from electrical stimulation of the cortex. These properties open up completely new possibilities for systematic scientific and clinical investigations of cortical connectivity (as depicted in Fig. 7) and cortical communication.

It appears useful to quantitatively compare the results of SIGNI to the more traditional CCEP method. Such a comparison is difficult, because the CCEP method is not standardized and it is not obvious which features of the ERP should be used for comparison. For example, ERP latency could be defined as the first time ERP amplitude is statistically different from a signal baseline or the time of the first positive/negative peak, etc. Likewise, ERP amplitude could be defined as the amplitude of the first peak, maximum peak-to-peak amplitude, an amplitude difference across specific peaks, etc. Fig. 8 illustrates this conundrum. The center panel shows the brain model for subject H. Each dot represents one of the implanted electrodes, the yellow circles give the electrodes

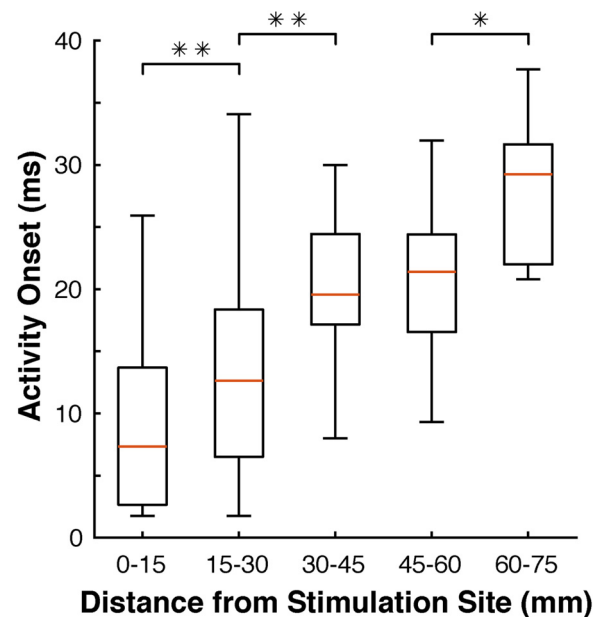


Fig. 6. Latency of broadband responses increases with distance from the stimulation site. Data are from all subjects, and responding electrodes are grouped by increments of 15 mm. Statistical significance (two-sample *t*-test) between adjacent groups is represented by a single ( $p < 0.05$ ) or double ( $p < 0.01$ ) asterisk.

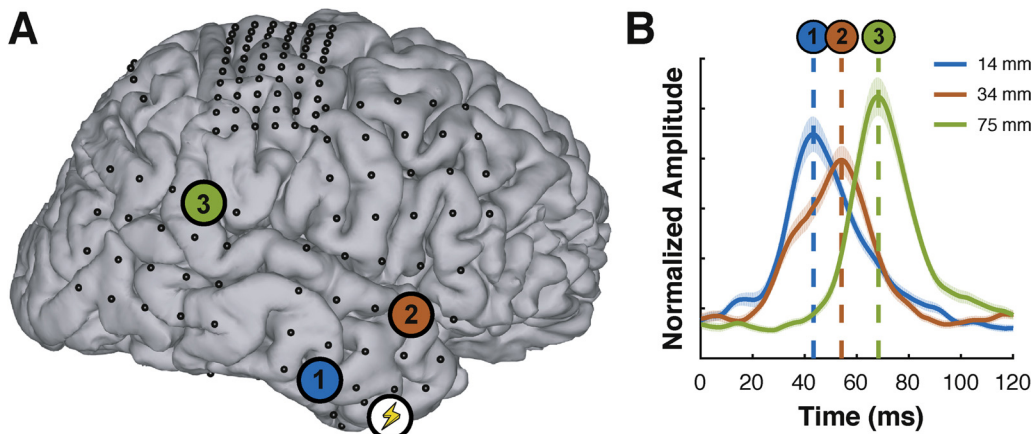
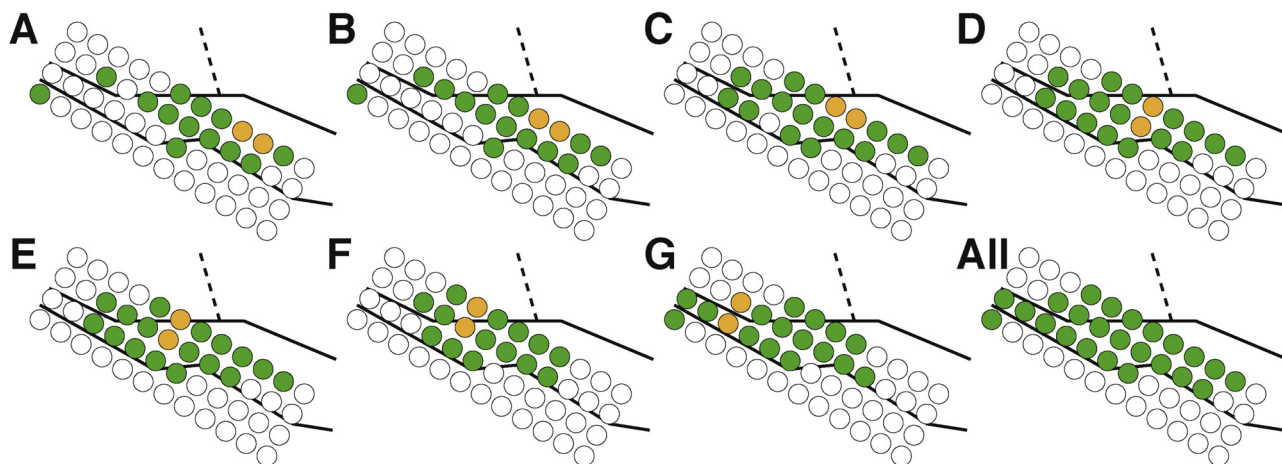


Fig. 5. Example of broadband responses at increasing distance from the stimulation site. (A) Cortical model and electrode locations (dots) from subject F. The location of stimulus delivery is marked with a lightning symbol. The locations of three responding sites are marked with colored circles numbered 1–3, respectively. (B) Broadband gamma time courses of these three locations. The peak of the evoked broadband gamma activity occurs later as distance to the stimulation site increases.



**Fig. 7.** Example of systematic study of cortical connectivity in superior temporal gyrus (right hemisphere) of subject H. (A–G) Electrical stimuli were delivered to seven electrode pairs on the depicted electrode array. Stimulated electrodes are shown in yellow, locations that exhibit a statistically significant response evaluated with SIGNI are shown in green. The underlying black lines indicate the approximate location of the superior temporal gyrus (solid lines) and central sulcus (dashed lines). All significant locations are indicated in the final panel.

that were stimulated in this example, and the labeled circles show the locations of electrodes with either ERP and/or broadband gamma responses to the stimuli (blue and red traces in surrounding plots, respectively). Broadband gamma responses can be assessed clearly by their amplitude and latency, and are absent in locations (such as middle temporal gyrus (F) or the frontal lobe (D and E)) that are known to not have direct connections to locations in superior temporal gyrus. In contrast, ERP responses have complex morphologies that differ across locations, and are present in all locations. Thus, this example, as well as the results from all locations from this subject shown in the Supplementary Material, makes it clear that there is little physiological justification for any attempt to quantify these ERP responses. Indeed, as described in the Introduction, these and other challenges provided the main motivation for the design of the SIGNI technique.

In our study, we evaluated the use of SIGNI with broadband gamma signals detected with electrophysiological techniques. With appropriate adaptations, it may also be applicable to single-neuron, DBS, or SEEG recordings or signals resulting from electrical, magnetic, or ultrasound stimulation, as well as from experiments using optogenetics.

SIGNI should be useful for basic neuroscience research, because it could contribute definitive evidence for end-to-endpoint connectivity between two distinct cortical areas, which is currently difficult to

establish with DTI and resting-state fMRI (Reveley et al., 2015 and Buckner et al. (2013), respectively). It could also help to elucidate the relationship between structural, functional, and effective connectivity, i.e., the extent to which cortical locations that support similar functions (such as speech processing) are more directly connected to each other even if they are spatially distant. SIGNI could also be useful for establishing the causal effect of low-frequency oscillatory activity in dynamically modulating the activity of the cortex. Although hundreds of studies have provided supporting evidence, the correlational or spatially non-specific nature of traditional methods (e.g., Wagner et al., 2007) have precluded definitive or specific conclusions.

Finally, SIGNI may also prove useful for clinical application in the context of invasive brain surgeries. For patients with epilepsy, it may aid in exploration of the epileptogenic network (Kamada et al., 2017; Spencer, 2002; Valentin et al., 2002). For resection of gray matter close to important white matter tracts, it may be useful to identify the cortical termini of those tracts. Indeed, just like with monitoring of EMG that is elicited by motor cortical stimulation, which is used to verify integrity of the spinal cord during surgery, it may be possible to monitor cortical responses to electrical stimulation to verify integrity of a particular white matter tract during resection. Finally, a general and important advantage of using electrical stimulation to map brain connectivity is

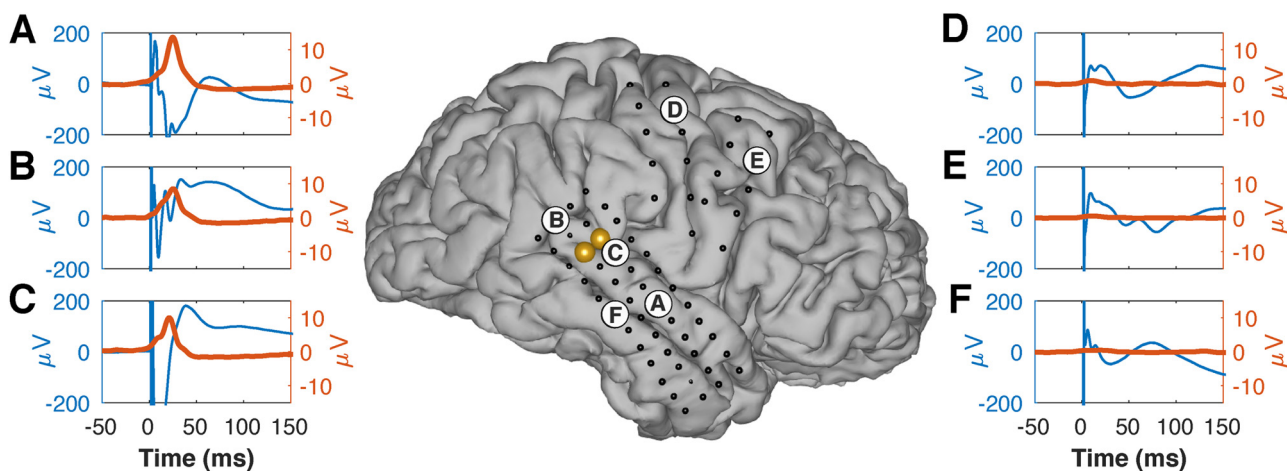


**Fig. 8.** Comparison of traditional evoked potentials (blue traces) and broadband gamma activity measured with SIGNI (red traces) for one stimulation pair (yellow dots) in subject H. (A–C) Locations that show broadband gamma responses to stimulation. Corresponding evoked potentials have complex and differing morphologies. (D–F) Locations that should not be anatomically connected to the sites in superior temporal gyrus, do not have broadband gamma responses, but do still show complex evoked responses.

that the subject does not need to engage in a particular task, which opens the tantalizing possibility that it may be feasible to apply it while the patient is under general anesthesia. This would be highly significant, as only a small minority of the 110,000 brain surgeries per year in the United States are performed with patients that are awake during parts of the surgery.

The results shown in this paper demonstrate that the use of SIGNI can produce results that cannot readily be achieved using traditional techniques. At the same time, our method does have distinct limitations. First, we currently disconnect the stimulated electrodes from the recording amplifier during stimulation. This greatly reduces artifacts, but prevents the study of activity at the site of stimulation. Second, our artifact removal procedure currently prevents analysis of cortical responses prior to 5 ms. Most of our responses occur at higher latencies, but the use of high-density electrode arrays with shorter electrode distances may require analyses closer to the time of stimulation. More generally, our approach is limited only to signals acquired using invasive methods. Furthermore, the implanted electrodes only cover a distinct fraction of the cortex, their location is different across subjects, and often only cover lateral parts of the cortex and not sulci or subcortical structures. Relatedly, SIGNI is useful only for determining end-to-end connectivity and not for identifying the location of the tracts connecting these endpoints. These unavoidable circumstances clearly limit the scientific or clinical questions that can be addressed using this approach.

## 5. Conclusion

The ability to provide definitive evidence for cortical connectivity through electrical stimulation provides scientists and clinicians with a powerful new tool. Our automated and quantitative method should facilitate rapid adoption of the technique. With these features, we expect that SIGNI will lead to new neuroscientific insights and will find utility in evaluations prior to invasive brain surgery.

## Acknowledgements

We thank Matthew Adamo and John Dalfino at the Department of Neurosurgery, Albany Medical College, for their contribution to this project. We also thank Nancy Kanwisher at MIT for her insightful comments during project-related discussions. This work was supported by grants from the National Institutes of Health (P41-EB018783, P50-MH109429), US Army Research Office (W911NF-14-1-0440), and Fondazione Neurone. This work was also supported by the Japanese government (Grant-in-Aid for Scientific Research (B) No. 16H05434, Grant-in-Aid for Exploratory Research No. 17H05900, and Grant-in-Aid for Scientific Research on Innovative Areas (Shintaisei System), JP 17K19708), and the European Union (Eurostars project RAPIDMAPS 2020 (ID 9273)). The authors have no conflict of interest, financial or otherwise, to declare.

## Appendix A. Supplementary data

Supplementary data associated with this article can be found, in the online version, at <https://doi.org/10.1016/j.jneumeth.2018.09.034>.

## References

Almashaikhi, T., Rheims, S., Ostrowsky-Coste, K., Montavont, A., Jung, J., De Bellecize, J., Arzimanoglou, A., Keo Kosal, P., Guénot, M., Bertrand, O., et al., 2014. Intralesional functional connectivity in human. *Hum. Brain Mapp.* 35 (6), 2779–2788.

Araki, K., Terada, K., Usui, K., Usui, N., Araki, Y., Baba, K., Matsuda, K., Tottori, T., Inoue, Y., 2015. Bidirectional neural connectivity between basal temporal and posterior language areas in humans. *Clin. Neurophysiol.* 126 (4), 682–688.

Assaf, Y., Pasternak, O., 2008. Diffusion tensor imaging (DTI)-based white matter mapping in brain research: a review. *J. Mol. Neurosci.* 34 (1), 51–61.

Brugge, J.F., Volkov, I.O., Garell, P.C., Reale, R.A., Howard, M.A., 2003. Functional connections between auditory cortex on Heschl's gyrus and on the lateral superior

temporal gyrus in humans. *J. Neurophysiol.* 90 (6), 3750–3763.

Buckner, R.L., Krienen, F.M., Yeo, B.T., 2013. Opportunities and limitations of intrinsic functional connectivity MRI. *Nat. Neurosci.* 16 (7), 832–837.

Catenoix, H., Magnin, M., Guénot, M., Isnard, J., Mauguier, F., Ryvlin, P., 2005. Hippocampal-orbitofrontal connectivity in human: an electrical stimulation study. *Clin. Neurophysiol.* 116 (8), 1779–1784.

Chang, E.F., Edwards, E., Nagarajan, S.S., Fogelson, N., Dalal, S.S., Canolty, R.T., Kirsch, H.E., Barbaro, N.M., Knight, R.T., 2011. Cortical spatio-temporal dynamics underlying phonological target detection in humans. *J. Cogn. Neurosci.* 23 (6), 1437–1446.

Conner, C.R., Ellmore, T.M., DiSano, M.A., Pieters, T.A., Potter, A.W., Tandon, N., 2011. Anatomic and electro-physiologic connectivity of the language system: a combined DTI-CCEP study. *Comput. Biol. Med.* 41 (12), 1100–1109.

Coon, W., Gunduz, A., Brunner, P., Ritaccio, A., Pesaran, B., Schalk, G., 2016. Oscillatory phase modulates the timing of neuronal activations and resulting behavior. *Neuroimage* 133, 294–301.

Coon, W., Schalk, G., 2016. A method to establish the spatiotemporal evolution of task-related cortical activity from electrocorticographic signals in single trials. *J. Neurosci. Methods* 271, 76–85.

Crone, N.E., Boatman, D., Gordon, B., Hao, L., 2001. Induced electrocorticographic gamma activity during auditory perception. *J. Clin. Neurophysiol.* 112 (4), 565–582.

Darvas, F., Scherer, R., Ojemann, J.G., Rao, R., Miller, K.J., Sorensen, L.B., 2010. High gamma mapping using EEG. *Neuroimage* 49 (1), 930–938.

David, O., Job, A.-S., De Palma, L., Hoffmann, D., Minotti, L., Kahane, P., 2013. Probabilistic functional tractography of the human cortex. *Neuroimage* 80, 307–317.

De Beeck, H.P.O., Haushofer, J., Kanwisher, N.G., 2008. Interpreting fMRI data: maps, modules and dimensions. *Nat. Rev. Neurosci.* 9 (2), 123–135.

Donos, C., Măliia, M.D., Mîndruță, I., Popa, I., Ene, M., Bălănescu, B., Ciurea, A., Barborica, A., 2016. A connectomics approach combining structural and effective connectivity assessed by intracranial electrical stimulation. *Neuroimage* 132, 344–358.

Edwards, E., Nagarajan, S.S., Dalal, S.S., Canolty, R.T., Kirsch, H.E., Barbaro, N.M., Knight, R.T., 2010. Spatiotemporal imaging of cortical activation during verb generation and picture naming. *Neuroimage* 50 (1), 291–301.

Edwards, E., Soltani, M., Deouell, L.Y., Berger, M.S., Knight, R.T., 2005. High gamma activity in response to deviant auditory stimuli recorded directly from human cortex. *J. Neurophysiol.* 94 (6), 4269–4280.

Edwards, E., Soltani, M., Kim, W., Dalal, S.S., Nagarajan, S.S., Berger, M.S., Knight, R.T., 2009. Comparison of time-frequency responses and the event-related potential to auditory speech stimuli in human cortex. *J. Neurophysiol.* 102 (1), 377–386.

Enatsu, R., Gonzalez-Martinez, J., Bulacio, J., Kubota, Y., Mosher, J., Burgess, R.C., Najm, I., Nair, D.R., 2015. Connections of the limbic network: a corticocortical evoked potentials study. *Cortex* 62, 20–33.

Enatsu, R., Kubota, Y., Kakisaka, Y., Bulacio, J., Piao, Z., O'Connor, T., Horning, K., Mosher, J., Burgess, R.C., Bingaman, W., et al., 2013a. Reorganization of posterior language area in temporal lobe epilepsy: a cortico-cortical evoked potential study. *Epilepsy Res.* 103 (1), 73–82.

Enatsu, R., Matsumoto, R., Piao, Z., O'Connor, T., Horning, K., Burgess, R.C., Bulacio, J., Bingaman, W., Nair, D.R., 2013b. Cortical negative motor network in comparison with sensorimotor network: a cortico-cortical evoked potential study. *Cortex* 49 (8), 2080–2096.

Engell, A.D., Huettel, S., McCarthy, G., 2012. The fMRI BOLD signal tracks electrophysiological spectral perturbations, not event-related potentials. *Neuroimage* 59 (3), 2600–2606.

Entz, L., Tóth, E., Keller, C.J., Bickel, S., Groppe, D.M., Fabó, D., Kozák, L.R., Erőss, L., Ulbert, I., Mehta, A.D., 2014. Evoked effective connectivity of the human neocortex. *Hum. Brain Mapp.* 35 (12), 5736–5753.

Formaggio, E., Storti, S., Tramontano, V., Casarin, A., Bertoldo, A., Fiaschi, A., Talacchi, A., Sala, F., Toffolo, G., Manganotti, P., 2013. Frequency and time-frequency analysis of intraoperative ECoG during awake brain stimulation. *Front. Neuroeng.* 6, 1.

Garell, P., Bakken, H., Greenlee, J., Volkov, I., Reale, R., Oya, H., Kawasaki, H., Howard, M., Brugge, J., 2012. Functional connection between posterior superior temporal gyrus and ventrolateral prefrontal cortex in human. *Cereb. Cortex* 23 (10), 2309–2321.

Greenlee, J.D., Oya, H., Kawasaki, H., Volkov, I.O., Kaufman, O.P., Kovach, C., Howard, M.A., Brugge, J.F., 2004. A functional connection between inferior frontal gyrus and orofacial motor cortex in human. *J. Neurophysiol.* 92 (2), 1153–1164.

Greenlee, J.D., Oya, H., Kawasaki, H., Volkov, I.O., Severson, M.A., Howard, M.A., Brugge, J.F., 2007. Functional connections within the human inferior frontal gyrus. *J. Comp. Neurol.* 503 (4), 550–559.

Hermes, D., Miller, K.J., Vansteensel, M.J., Aarnoutse, E.J., Leijten, F.S., Ramsey, N.F., 2012. Neurophysiologic correlates of fMRI in human motor cortex. *Hum. Brain Mapp.* 33 (7), 1689–1699.

Howard, M.A., Volkov, I., Mirsky, R., Garell, P., Noh, M., Granner, M., Damasio, H., Steinschneider, M., Reale, R., Hind, J., et al., 2000. Auditory cortex on the human posterior superior temporal gyrus. *J. Comp. Neurol.* 416 (1), 79–92.

Jensen, O., Kaiser, J., Lachaux, J.-P., 2007. Human gamma-frequency oscillations associated with attention and memory. *Trends Neurosci.* 30 (7), 317–324.

Jiménez-Jiménez, D., Abete-Rivas, M., Martín-López, D., Lacruz, M.E., Selway, R.P., Valentín, A., Alarcón, G., 2015. Incidence of functional bi-temporal connections in the human brain in vivo and their relevance to epilepsy surgery. *Cortex* 65, 208–218.

Kam, J., Szczepanski, S., Canolty, R., Flinker, A., Augustine, K., Crone, N., Kirsch, H., Kuperman, R., Lin, J., Parvizi, J., et al., 2016. Differential sources for 2 neural signatures of target detection: an electrocorticography study. *Cereb. Cortex* 1–12.

Kamada, K., Ogawa, H., Kapeller, C., Prueckl, R., Hiroshima, S., Tamura, Y., Takeuchi, F., Guger, C., 2017. Disconnection of the pathological connectome for multifocal epilepsy surgery. *J. Neurosurg.* 1–13.

- Keller, C.J., Bickel, S., Entz, L., Ulbert, I., Milham, M.P., Kelly, C., Mehta, A.D., 2011. Intrinsic functional architecture predicts electrically evoked responses in the human brain. *Proc. Natl. Acad. Sci.* 108 (25), 10308–10313.
- Keller, C.J., Honey, C.J., Entz, L., Bickel, S., Groppe, D.M., Toth, E., Ulbert, I., Lado, F.A., Mehta, A.D., 2014a. Corticocortical evoked potentials reveal projectors and integrators in human brain networks. *J. Neurosci.* 34 (27), 9152–9163.
- Keller, C.J., Honey, C.J., Mégevand, P., Entz, L., Ulbert, I., Mehta, A.D., 2014b. Mapping human brain networks with cortico-cortical evoked potentials. *Philos. Trans. R. Soc. B* 369 (1653), 20130528.
- Kikuchi, T., Matsumoto, R., Mikuni, N., Yokoyama, Y., Matsumoto, A., Ikeda, A., Fukuyama, H., Miyamoto, S., Hashimoto, N., 2012. Asymmetric bilateral effect of the supplementary motor area proper in the human motor system. *Clin. Neurophysiol.* 123 (2), 324–334.
- Koubeissi, M.Z., Lesser, R.P., Sinai, A., Gaillard, W.D., Franzczuk, P.J., Crone, N.E., 2011. Connectivity between perisylvian and bilateral basal temporal cortices. *Cereb. Cortex* 22 (4), 918–925.
- Kubaneck, J., Schalk, G., 2015. NeuralAct: a tool to visualize electrocortical (ECoG) activity on a three-dimensional model of the cortex. *Neuroinformatics* 13 (2), 167–174.
- Lacruz, M., Garcia Seoane, J., Valentin, A., Selway, R., Alarcon, G., 2007. Frontal and temporal functional connections of the living human brain. *Eur. J. Neurosci.* 26 (5), 1357–1370.
- Lacuey, N., Zonjy, B., Kahrman, E.S., Kaffashi, F., Miller, J., Lüders, H.O., 2015. Functional connectivity between right and left mesial temporal structures. *Brain Struct. Funct.* 220 (5), 2617–2623.
- Logothetis, N.K., Pauls, J., Augath, M., Trinath, T., Oeltermann, A., 2001. Neurophysiological investigation of the basis of the fMRI signal. *Nature* 412 (6843), 150–157.
- Makeig, S., Westerfield, M., Jung, T.-P., Enghoff, S., Townsend, J., Courchesne, E., Sejnowski, T.J., 2002. Dynamic brain sources of visual evoked responses. *Science* 295 (5555), 690–694.
- Manning, J.R., Jacobs, J., Fried, I., Kahana, M.J., 2009. Broadband shifts in local field potential power spectra are correlated with single-neuron spiking in humans. *J. Neurosci.* 29 (43), 13613–13620.
- Maris, E., van Vugt, M., Kahana, M., 2011. Spatially distributed patterns of oscillatory coupling between high-frequency amplitudes and low-frequency phases in human iEEG. *Neuroimage* 54 (2), 836–850.
- Massey, F.J., 1951. The Kolmogorov-Smirnov test for goodness of fit. *J. Am. Stat. Assoc.* 46 (253), 68–78.
- Matsumoto, R., Nair, D.R., Ikeda, A., Fumuro, T., LaPresto, E., Mikuni, N., Bingaman, W., Miyamoto, S., Fukuyama, H., Takahashi, R., et al., 2012. Parieto-frontal network in humans studied by cortico-cortical evoked potential. *Hum. Brain Mapp.* 33 (12), 2856–2872.
- Matsumoto, R., Nair, D.R., LaPresto, E., Bingaman, W., Shibasaki, H., Lüders, H.O., 2007. Functional connectivity in human cortical motor system: a cortico-cortical evoked potential study. *Brain* 130 (1), 181–197.
- Matsumoto, R., Nair, D.R., LaPresto, E., Najm, I., Bingaman, W., Shibasaki, H., Lüders, H.O., 2004. Functional connectivity in the human language system: a cortico-cortical evoked potential study. *Brain* 127 (10), 2316–2330.
- Matsuzaki, N., Juhász, C., Asano, E., 2013. Cortico-cortical evoked potentials and stimulation-elicited gamma activity preferentially propagate from lower- to higher-order visual areas. *Clin. Neurophysiol.* 124 (7), 1290–1296.
- Mazaheri, A., Jensen, O., 2006. Posterior  $\alpha$  activity is not phase-reset by visual stimuli. *Proc. Natl. Acad. Sci.* 103 (8), 2948–2952.
- Mazaheri, A., Jensen, O., 2008. Asymmetric amplitude modulations of brain oscillations generate slow evoked responses. *J. Neurosci.* 28 (31), 7781–7787.
- Miller, K.J., Sorensen, L.B., Ojemann, J.G., den Nijs, M., 2009. Power-law scaling in the brain surface electric potential. *PLoS Comput. Biol.* 5 (12), e1000609.
- Mukamel, R., Gelbard, H., Arieli, A., Hasson, U., Fried, I., Malach, R., 2005. Coupling between neuronal firing, field potentials, and fMRI in human auditory cortex. *Science* 309 (5736), 951–954.
- Niessing, J., Ebisch, B., Schmidt, K.E., Niessing, M., Singer, W., Galuske, R.A., 2005. Hemodynamic signals correlate tightly with synchronized gamma oscillations. *Science* 309 (5736), 948–951.
- Oya, H., Poon, P.W., Brugge, J.F., Reale, R.A., Kawasaki, H., Volkov, I.O., Howard, M.A., 2007. Functional connections between auditory cortical fields in humans revealed by Granger causality analysis of intra-cranial evoked potentials to sounds: comparison of two methods. *Biosystems* 89 (1), 198–207.
- Ray, S., Maunsell, J., 2011. Different origins of gamma rhythm and high-gamma activity in macaque visual cortex. *PLoS Biol.* 9 (4), e1000610.
- Ray, S., Niebur, E., Hsiao, S.S., Sinai, A., Crone, N.E., 2008. High-frequency gamma activity (80–150 Hz) is increased in human cortex during selective attention. *Clin. Neurophysiol.* 119 (1), 116–133.
- Reveley, C., Seth, A.K., Pierpaoli, C., Silva, A.C., Yu, D., Saunders, R.C., Leopold, D.A., Frank, Q.Y., 2015. Superficial white matter fiber systems impede detection of long-range cortical connections in diffusion MR tractography. *Proc. Natl. Acad. Sci.* 112 (21), E2820–E2828.
- Rosenberg, D., Manguiere, F., Catenoix, H., Faillenot, I., Magnin, M., 2008. Reciprocal thalamocortical connectivity of the medial pulvinar: a depth stimulation and evoked potential study in human brain. *Cereb. Cortex* 19 (6), 1462–1473.
- Saito, T., Tamura, M., Muragaki, Y., Maruyama, T., Kubota, Y., Fukuchi, S., Nitta, M., Chernov, M., Okamoto, S., Sugiyama, K., et al., 2014. Intraoperative cortico-cortical evoked potentials for the evaluation of language function during brain tumor resection: initial experience with 13 cases. *J. Neurosurg.* 121 (4), 827–838.
- Schalk, G., Kapeller, C., Guger, C., Ogawa, H., Hiroshima, S., Lafer-Sousa, R., Saygin, Z.M., Kamada, K., Kanwisher, N., 2017. Facephens and rainbows: causal evidence for functional and anatomical specificity of face and color processing in the human brain. *Proc. Natl. Acad. Sci.* 114 (46), 12285–12290.
- Schalk, G., Kubaneck, J., Miller, K., Anderson, N., Leuthardt, E., Ojemann, J., Limbrick, D., Moran, D., Gerhardt, L., Wolpaw, J., 2007. Decoding two-dimensional movement trajectories using electrocorticographic signals in humans. *J. Neural Eng.* 4 (3), 264.
- Schalk, G., McFarland, D.J., Hinterberger, T., Birbaumer, N., Wolpaw, J.R., 2004. BCI2000: a general-purpose brain-computer interface (BCI) system. *IEEE Trans. Biomed. Eng.* 51 (6), 1034–1043.
- Schalk, G., Mellinger, J., 2010. A Practical Guide to Brain-Computer Interfacing with BCI2000: General-Purpose Software for Brain-Computer Interface Research, Data Acquisition, Stimulus Presentation, and Brain Monitoring. Springer Science & Business Media.
- Smith, S.M., Vidaurre, D., Beckmann, C.F., Glasser, M.F., Jenkinson, M., Miller, K.L., Nichols, T.E., Robinson, E.C., Salimi-Khorshidi, G., Woolrich, M.W., et al., 2013. Functional connectomes from resting-state fMRI. *Trends Cogn. Sci.* 17 (12), 666–682.
- Spencer, S.S., 2002. Neural networks in human epilepsy: evidence of and implications for treatment. *Epilepsia* 43 (3), 219–227.
- Swann, N.C., Cai, W., Conner, C.R., Pieters, T.A., Claffey, M.P., George, J.S., Aron, A.R., Tandon, N., 2012. Roles for the pre-supplementary motor area and the right inferior frontal gyrus in stopping action: electrophysiological responses and functional and structural connectivity. *Neuroimage* 59 (3), 2860–2870.
- Tamura, Y., Ogawa, H., Kapeller, C., Prueckl, R., Takeuchi, F., Anei, R., Ritaccio, A., Guger, C., Kamada, K., 2016. Passive language mapping combining real-time oscillation analysis with cortico-cortical evoked potentials for awake craniotomy. *J. Neurosurg.* 125 (6), 1580–1588.
- Terada, K., Umeoka, S., Usui, N., Baba, K., Usui, K., Fujitani, S., Matsuda, K., Tottori, T., Nakamura, F., Inoue, Y., 2012. Uneven interhemispheric connections between left and right primary sensori-motor areas. *Hum. Brain Mapp.* 33 (1), 14–26.
- Terada, K., Usui, N., Umeoka, S., Baba, K., Mihara, T., Matsuda, K., Tottori, T., Agari, T., Nakamura, F., Inoue, Y., 2008. Interhemispheric connection of motor areas in humans. *J. Clin. Neurophysiol.* 25 (6), 351–356.
- Tort, A.B., Kramer, M.A., Thorn, C., Gibson, D.J., Kubota, Y., Graybiel, A.M., Kopell, N.J., 2008. Dynamic cross-frequency couplings of local field potential oscillations in rat striatum and hippocampus during performance of a t-maze task. *Proc. Natl. Acad. Sci.* 105 (51), 20517–20522.
- Trebaul, L., Rudrauf, D., Job, A.-S., Mälfia, M.D., Popa, I., Barborica, A., Minotti, L., Mündrūt, I., Kahane, P., David, O., 2016. Stimulation artifact correction method for estimation of early cortico-cortical evoked potentials. *J. Neurosci. Methods* 264, 94–102.
- Umeoka, S., Terada, K., Baba, K., Usui, K., Matsuda, K., Tottori, T., Usui, N., Nakamura, F., Inoue, Y., Fujiwara, T., et al., 2009. Neural connection between bilateral basal temporal regions: cortico-cortical evoked potential analysis in patients with temporal lobe epilepsy. *Neurosurgery* 64 (5), 847–855.
- Valentin, A., Anderson, M., Alarcon, G., Seoane, J.G., Selway, R., Binnie, C., Polkey, C., 2002. Responses to single pulse electrical stimulation identify epileptogenesis in the human brain in vivo. *Brain* 125 (8), 1709–1718.
- Voytek, B., Secundo, L., Bidet-Caulet, A., Scabini, D., Stiver, S.I., Gean, A.D., Manley, G.T., Knight, R.T., 2010. Hemicraniectomy: a new model for human electrophysiology with high spatio-temporal resolution. *J. Cogn. Neurosci.* 22 (11), 2491–2502.
- Wagner, T., Valero-Cabre, A., Pascual-Leone, A., 2007. Noninvasive human brain stimulation. *Annu. Rev. Biomed. Eng.* 9, 527–565.
- Wang, W., Collinger, J.L., Perez, M.A., Tyler-Kabara, E.C., Cohen, L.G., Birbaumer, N., Brose, S.W., Schwartz, A.B., Boninger, M.L., Weber, D.J., 2010. Neural interface technology for rehabilitation: exploiting and promoting neuroplasticity. *Phys. Med. Rehabil. Clin. N. Am.* 21 (1), 157–178.
- Whittingstall, K., Logothetis, N.K., 2009. Frequency-band coupling in surface EEG reflects spiking activity in monkey visual cortex. *Neuron* 64 (2), 281–289.
- Wilson, C., Isokawa, M., Babb, T., Crandall, P., 1990. Functional connections in the human temporal lobe. *Exp. Brain Res.* 82 (2), 279–292.
- Wilson, C., Isokawa, M., Babb, T., Crandall, P., Levesque, M., Engel Jr., J., 1991. Functional connections in the human temporal lobe. II. Evidence for a loss of functional linkage between contralateral limbic structures. *Exp. Brain Res.* 85 (1), 174–187.
- Yamao, Y., Matsumoto, R., Kunieda, T., Arakawa, Y., Kobayashi, K., Usami, K., Shibata, S., Kikuchi, T., Sawamoto, N., Mikuni, N., et al., 2014. Intraoperative dorsal language network mapping by using single-pulse electrical stimulation. *Hum. Brain Mapp.* 35 (9), 4345–4361.